

Coordinate System Influence on the Regularized Trajectory Optimization Problem

J. M. LEWALLEN*

NASA Manned Spacecraft Center, Houston, Texas

AND

O. A. SCHWAUSCH†

Lockheed Electronics Company, Houston, Texas

AND

B. D. TAPLEY‡

The University of Texas at Austin, Austin, Texas

The use of regularized variables to enhance the numerical integration process associated with the optimal trajectory of a continuously thrusting space vehicle is evaluated. Both rectangular Cartesian and polar cylindrical coordinates are considered for an optimal low-thrust Earth-escape spiral trajectory and an optimal low-thrust Earth-Jupiter transfer trajectory. The results obtained indicate that (for space vehicles which experience wide variations in the gravitational force magnitude) significant reductions (up to 67%) in computing time can be obtained by using the regularized trajectory optimization equations. For the problems considered here, the polar coordinates give shorter times, and are less sensitive to errors in the initial Lagrange multipliers, than the rectangular coordinates. If the numerically evaluated Hamiltonian (which is theoretically constant) is used as an indication of integration error generation, the tradeoff between integration time and integration error becomes apparent.

Introduction

DURING the past decade, considerable effort has been directed toward determining numerical methods for optimization of nonlinear dynamic systems. The characteristics of several of the more popular direct and indirect numerical optimization methods are compared in Ref. 1, and the procedures for accelerating convergence of the indirect optimization methods are discussed in Ref. 2. The primary consideration in evaluating an optimization method is the computing time required for convergence to a sufficiently accurate solution. These characteristics may be influenced by the functional form of the equations of motion, as well as by the choice of the coordinate system. The numerical integration characteristics can be enhanced considerably when a regularized set of differential equations is used for trajectories that experience close primary body approaches,³ or for a wide range of problems in celestial mechanics.⁴ Based on these conclusions, a study was made to determine the feasibility of using regularizing transformations to improve the computational characteristics of numerical optimization procedures. Some numerical results⁵ indicate significant numerical advantages in terms of computational time and accuracy of terminal condition satisfaction.

The effect of the regularizing transformation on time and accuracy of the numerical solution is dependent on the choice

of the coordinate system for the unregularized variables, as noted for the two-body problem in Ref. 6, and for the trajectory optimization problem in Refs. 7 and 8. These investigations revealed that the polar coordinates are computationally superior to the rectangular coordinates for the continuously powered escape spiral.

In this paper the effects of using rectangular Cartesian and polar cylindrical coordinate systems are considered for a minimum time low-thrust Earth-escape spiral trajectory and a minimum time Earth-Jupiter transfer trajectory, for various bounds on the single-step integration error.

Formulation

If the transfer trajectory for a continuously powered low-thrust space vehicle is to be time optimal, the following equations must be satisfied in the interval $t_0 \leq t \leq t_f$

$$\ddot{\bar{r}} = -\mu (\bar{r}/r^3) - T\bar{\lambda}/m\lambda, \dot{m} = -\beta \quad (1)$$

and

$$\ddot{\bar{\lambda}} = -\mu (\bar{\lambda}/r^3) + 3\mu [(\bar{\lambda} \cdot \bar{r})/r^5]\bar{r}, \dot{\lambda}_m = -T\lambda/m^2 \quad (2)$$

Here the mass is $m = m_0 - \beta t$ where β is a constant mass-flow rate and $\bar{\lambda}$ and $\bar{\omega}$ are Lagrange multiplier vectors. The boundary conditions that must be satisfied are

$$\bar{r}(t_0) = \bar{r}_0, \bar{v}(t_0) = \bar{v}_0, m(t_0) = m_0 \quad (3)$$

$$\bar{r}(t_f) = \bar{r}_f, \bar{v}(t_f) = \bar{v}_f, \lambda_m(t_f) = 0 \quad (4)$$

and

$$1 + \bar{\lambda} \cdot \left[-\mu \frac{\bar{r}}{r^3} - \frac{T\bar{\lambda}}{m\lambda} \right] + \bar{\omega} \cdot \bar{v} - \lambda_m \beta \Big|_{t_f} = 0 \quad (5)$$

Presented as Paper 69-903 at the AIAA/AAS Astrodynamics Conference, Princeton, N. J., August 20-22, 1969; submitted September 24, 1969; revision received August 28, 1970.

* Chief, Mission Planning and Analysis Division. Member AIAA.

† Senior Scientific Programmer. Member AIAA.

‡ Chairman and Professor, Department of Aerospace Engineering. Member AIAA.

where r is the radius vector, μ is the universal gravitational constant, T is the spacecraft thrust, and v is the spacecraft velocity. By using a generalization of the classical Sundman regularizing transformation⁹

$$d\tau = r^{-3/2} dt \quad (6)$$

a set of regularized equations for the optimal trajectory can be obtained as follows:

$$\ddot{\bar{r}}'' = \frac{3}{2}(\bar{r} \cdot \bar{r}')\bar{r}'/r^2 - \mu\bar{r} - Tr^2\bar{\lambda}/m\lambda, \quad m' = -\beta r^{3/2} \quad (7)$$

and

$$\ddot{\bar{\lambda}}'' = \frac{3}{2}(\bar{r} \cdot \bar{r}')\bar{\lambda}'/r^2 - \mu\bar{\lambda} + 3\mu\frac{(\bar{\lambda} \cdot \bar{r})\bar{r}}{r^2}, \quad \lambda_m' = -\frac{Tr^{3/2}\lambda}{m^2} \quad (8)$$

The primes indicate derivatives with respect to the pseudo-time variable τ rather than the real time t . This transformation is discussed in Ref. 5 where the Eqs. (7) and (8) are shown to be mathematically regular. This vector form of the regularized equations is invariant with the choice of coordinate system. Hence, Eqs. (1) and (2) describe the optimal process in the unregularized rectangular and polar coordinates, while Eqs. (7) and (8) describe the regularized equations associated with each of the coordinate systems. The usual nonlinear two-point boundary value problem can be represented by either set of equations.

Discussions of Results

To solve the optimal trajectory problem, efforts usually are made to obtain a numerical solution to Eqs. (1) and (2), which satisfies the boundary conditions given by Eqs. (3-5). Since only one-half of the necessary initial conditions are specified in Eq. (3), values for the remaining unknown initial conditions (usually Lagrange multipliers and the unknown time) must be assumed before a numerical solution can be determined. Inasmuch as the values of the unknown initial boundary conditions are arbitrarily selected, the terminal constraints given by Eqs. (4) and (5) will not be satisfied. These arbitrarily selected initial conditions are changed systematically on subsequent iterations¹ until the norm of the terminal constraint error is less than 10^{-7} . Sufficient numerical accuracy is obtained by using full double precision arithmetic on the UNIVAC 1108 at the NASA Manned Spacecraft Center, and by performing the integrations with a variable stepsize integration scheme, thereby maintaining

the single-step error within certain desired tolerance limits. A fourth-order Runge-Kutta starter and a fourth-order Adams-Bashforth predictor corrector are used.¹⁰

The chosen low-thrust trajectories are appropriate for regularization investigations, since the gravitational force magnitude varies by approximately 10^2 ; thus, it is expected that a wide range of numerical integration stepsizes will be required to maintain certain specified error bounds. The optimal Earth-escape spiral trajectory is shown in Fig. 1. Initially, the spacecraft is in a circular near-Earth orbit with a radius equal to 1.05 times the radius of the Earth. For a constant low-thrust space vehicle subjected to an initial T/m of 0.1, the spacecraft acquires escape energy in approximately 70 normalized time units (approximately 15.7 hr) and reaches an orbit of radius equal to 8.5 times the radius of the Earth. Although this T/m is relatively large, it represents a compromise between a computationally expensive realistic trajectory and an inexpensive unrealistic trajectory. The optimal control programs for both the rectangular and polar coordinate systems are shown in Fig. 1. The relationship between the real and regularized time for the optimal trajectory is shown in Fig. 2.

Integration characteristics for single-step integration error-bound separations are 10^6 , 10^4 , and 10^2 , for parts a, b, and c of Table 1, respectively. Here Σ represents the computation time needed to integrate the state equations, the Euler-Lagrange equations, and the perturbation equations from the initial time to the final time, plus the time required to monitor the single-step integration error and to determine the appropriate integration stepsize. The appropriate stepsize is determined by comparing the single-step error with the desired accuracy limits. If either the maximum or minimum error limit is encountered, the stepsize is either halved or doubled. If, by doubling the stepsize, the maximum bound is violated, then the stepsize remains unchanged. Also, the number of integration steps n taken in the interval and the number of stepsize changes, m necessary to maintain the desired accuracy are recorded. No distinction is made in the tables between changes associated with doubling and halving the stepsize. The average computer time t_m for each integration step is recorded to indicate the degree of complexity of the equations for each case. The norm of the constraint error \bar{e}_f should be considered with some reservation, since the routine simply requires that the norm be less than 10^{-7} . The extent to which this criterion is exceeded is not controlled and is an indication of the convergence rate; however, it also depends on how close the terminal norm for the previous iteration was to the required value of 10^{-7} .

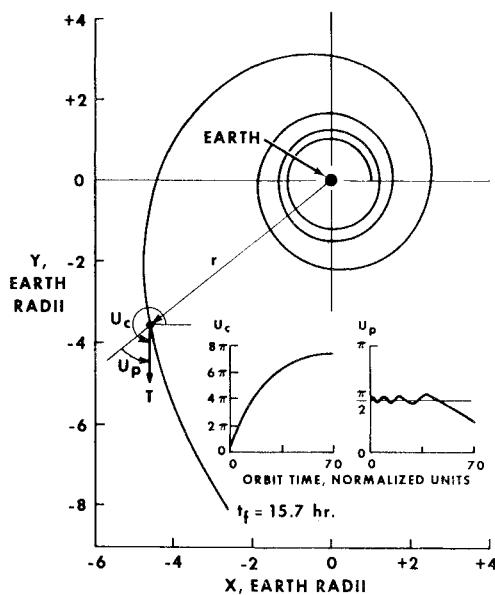


Fig. 1 Optimal low-thrust Earth-escape spiral trajectory for $T/m = 0.1$.

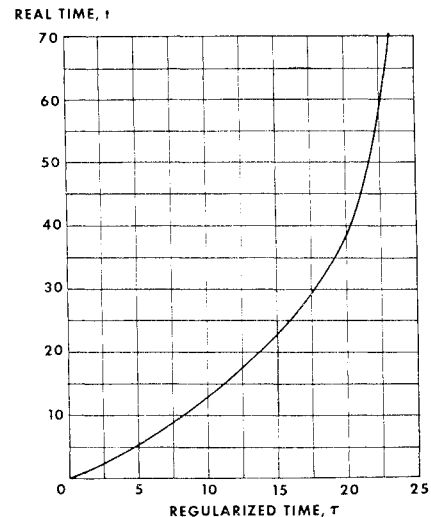


Fig. 2 Real time compared to regularized time for the optimal low-thrust Earth-escape spiral trajectory.

The results presented in part "a" of Table 1 are for the relatively large error-bound separation of 10^6 . The regularized variables (in either coordinate system) require less computation time for each iteration than the unregularized variables. In some cases, the time is reduced by a factor of 3. The reason for the large saving in time is apparent when both t_m and n are examined. Although evaluation times are

Table 1 Numerical integration characteristics for the optimal low-thrust Earth-escape spiral^a

	Maximum Allowable error (absolute)	Unregularized		Regularized	
		Rectangular	Polar	Rectangular	Polar
a) For error-bound separation of 10^6					
Σ sec	10^{-4}	19.5	20.6	8.3	7.7
	10^{-6}	30.0	21.0	15.2	8.1
	10^{-8}	71.1	42.5	29.4	15.6
tm , msec		0.0275	0.0300	0.0304	0.0307
n	10^{-4}	702	685	272	251
	10^{-6}	1381	702	497	261
	10^{-8}	2594	1403	971	508
m	10^{-4}	0	1	1	1
	10^{-6}	2	0	2	2
	10^{-8}	3	1	2	2
$\bar{e}f$	10^{-4}	1.375^{-9}	4.365^{-12}	6.228^{-10}	9.087^{-11}
	10^{-6}	1.524^{-10}	3.681^{-12}	9.438^{-8}	8.325^{-11}
	10^{-8}	2.010^{-10}	5.336^{-8}	1.330^{-7}	2.150^{-10}
b) For error-bound separation of 10^4					
Σ sec	10^{-4}	16.4	13.9	8.4	7.7
	10^{-5}	27.8	18.2	15.2	8.1
	10^{-6}	51.2	31.8	30.1	15.7
	10^{-7}	64.0	37.7	34.0	21.7
	10^{-8}	108.6	72.4	60.1	32.1
tm , msec		0.0276	0.0299	0.0307	0.0310
n	10^{-4}	585	460	272	251
	10^{-5}	993	606	497	261
	10^{-6}	1862	1080	971	508
	10^{-7}	2327	1254	1088	709
	10^{-8}	3957	2417	1991	1049
m	10^{-4}	2	2	1	1
	10^{-5}	3	1	2	2
	10^{-6}	4	3	2	2
	10^{-7}	4	2	3	3
	10^{-8}	5	3	4	4
$\bar{e}f$	10^{-4}	5.603^{-9}	1.265^{-9}	6.228^{-10}	9.087^{-11}
	10^{-5}	1.849^{-10}	5.304^{-12}	9.438^{-8}	8.325^{-11}
	10^{-6}	1.766^{-10}	5.328^{-8}	1.330^{-7}	2.510^{-11}
	10^{-7}	1.413^{-10}	5.336^{-10}	1.244^{-7}	2.406^{-10}
	10^{-8}	1.378^{-10}	6.035^{-8}	1.258^{-7}	2.042^{-10}
c) For error-bound separation of 10^2					
Σ sec	10^{-4}	9.4	7.5	8.3	6.1
	10^{-5}	17.3	10.6	15.4	8.1
	10^{-6}	26.6	15.5	30.1	15.7
	10^{-7}	36.4	26.3	33.8	21.7
	10^{-8}	66.8	40.6	61.6	32.6
	10^{-9}	105.5	60.7	119.1	61.2
	10^{-10}	147.1	102.5	132.7	77.8
tm , msec		0.0279	0.0301	0.0307	0.0307
n	10^{-4}	332	241	272	193
	10^{-5}	611	345	497	261
	10^{-6}	954	514	971	508
	10^{-7}	1314	869	1088	709
	10^{-8}	2423	1363	1991	1049
	10^{-9}	3757	2039	3884	2038
	10^{-10}	5235	3467	4355	2582
m	10^{-4}	3	3	1	3
	10^{-5}	4	3	2	2
	10^{-6}	6	4	2	2
	10^{-7}	5	3	3	3
	10^{-8}	6	5	4	4
	10^{-9}	8	6	4	5
	10^{-10}	7	5	5	5
$\bar{e}f$	10^{-4}	2.197^{-7}	9.750^{-12}	6.228^{-10}	1.527^{-12}
	10^{-5}	1.515^{-9}	1.676^{-7}	9.438^{-8}	8.325^{-11}
	10^{-6}	1.826^{-9}	2.231^{-8}	1.329^{-8}	2.150^{-10}
	10^{-7}	2.580^{-10}	5.122^{-8}	1.244^{-7}	2.406^{-10}
	10^{-8}	1.133^{-10}	5.962^{-8}	1.258^{-7}	2.042^{-10}
	10^{-9}	1.624^{-10}	6.061^{-8}	1.260^{-7}	2.054^{-10}
	10^{-10}	1.560^{-9}	6.081^{-8}	1.259^{-7}	2.005^{-10}

^a Σ = Computation time for integration of state and perturbation equations, sec; t_m = mean computation time per integration step, msec; n = number of integration steps; m = number of stepsize changes; and $\bar{e}f$ = terminal error norm.

larger for the regularized equations, the n 's are much smaller. The polar coordinates generally require less computer time than the rectangular coordinates.

The results shown in part b of Table 1 for an error-bound separation of 10^4 agree with the results presented in part a and substantiate the previous conclusions, but the computation time advantage of the regularized systems has been reduced slightly; and the differences in n are smaller. In addition, m is smaller for the regularized variables than for the unregularized variables; in keeping with the theory that predicts that regularized variables will undergo fewer stepsize changes provided that a certain integration accuracy is maintained. (For the previous error-bound separation of 10^6 , a comparison of m 's is invalid, since, in some instances, the lower error bound was never encountered.)

The results in part c of Table 1 for the error-bound separation of 10^2 generally agree with the results in parts a and b, but for this magnitude of error-bound separation, the integration times for the regularized and unregularized variables are essentially the same. The departures from the noted trend are explained in Fig. 3, wherein the top line in each set of four lines represents the maximum allowable error bound. Each succeeding line represents the minimum allowable error for a particular error-bound separation. Thus, the first set of four lines represents the integration error bounds of 10^{-4} - 10^{-6} , 10^{-4} - 10^{-8} , and 10^{-4} - 10^{-10} . The boundary encounters are plotted vs normalized trajectory time. The encounter of the numerical error magnitude with either of the boundaries is recorded by the appropriate symbol (keyed in Fig. 3). The stepsize will be doubled if the lower boundary is encountered; the stepsize will be halved if the upper boundary is encountered.

By maintaining the small integration error-bound separation of 10^2 , the error in the unregularized rectangular variables is such that the stepsize is doubled three times during the escape trajectory for the 10^{-4} - 10^{-6} accuracy limits (Fig. 3.) By increasing the error separation to 10^4 (to give error bounds of 10^{-4} - 10^{-8}), the unregularized rectangular error crosses the minimum acceptable error bound only twice. The first encounter with the 10^{-8} boundary comes after the 10^{-6} boundary, in the previous case, had already been crossed twice. By doubling the stepsize early in the trajectory flight time, requiring the rectangular error to be within the 10^{-4} - 10^{-6} accuracy levels rather than within the 10^{-4} - 10^{-8} accuracy levels, 253 integration steps were eliminated, saving 7 sec of computer time for each iteration. Likewise, by requiring the integration error to be within the 10^{-4} - 10^{-6}

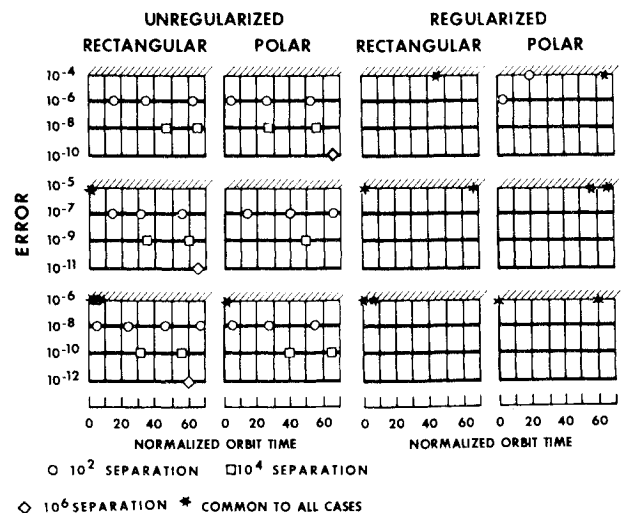


Fig. 3 Integration error-boundary encounters for various error-bound separations for the optimal low-thrust Earth-escape spiral.

accuracy levels rather than with the 10^{-4} - 10^{-10} accuracy levels, a 10-sec saving in computer time for each iteration was realized. This same trend appeared in both the rectangular and polar coordinates for the other error bounds shown. By maintaining the integration error within the smaller error bounds, the total integration time was reduced and made comparable to that for the regularized system.

Integration errors in the regularized coordinate systems propagate differently than do errors in the unregularized coordinate systems (Fig. 3). Since a feature of regularization is the automatic scaling of integration stepsize in real time, an increasing radius vector magnitude will increase automatically the stepsize, whereas a decreasing radius vector magnitude will decrease it. For the Earth-escape spiral trajectory, the radius vector is continually increasing; therefore, the stepsize may be reduced to maintain the desired accuracy. With only one exception, the integration stepsize for the regularized variables is always halved (Fig. 3). The exception occurs for the 10^{-4} - 10^{-6} accuracy levels, using the polar coordinates. In this case, the error is such that 10^{-6} boundary is just crossed, thereby doubling the stepsize. With further integration, the error is increased, and the stepsize is halved again. In all other instances, the lower boundaries are never encountered. Since the lower boundaries are not encountered, increasing the error-bound separation limit does not affect the regularized systems and only penalizes the unregularized system by increasing the integration times.

In the minimum time Earth-Jupiter transfer, Fig. 4, the magnitude of the position vector decreases and then increases. The initial position and velocity of the spacecraft for this case correspond to the position and velocity of the Earth on December 1, 1983. For a spacecraft with a constant thrust of 0.24497×10^{-4} normalized units, the transfer takes approximately 905 days. The representative numerical results in Table 2 show the computational characteristics of the various formulations for a constant error-bound separation of 10^4 . The regularized variables exhibit shorter computational times than the unregularized variables in all the cases

considered; the polar coordinates, shorter times than the rectangular coordinates. These trends were maintained for the other error-bound separations considered.

The integration error-boundary encounters for various boundary separations are presented in Fig. 5, and the reason for the computational advantage with regularized coordinate systems can be seen. The region of particular interest is the time period between 300 and 400 days, during which the close approach to the sun is made (Fig. 4). During this interval, the unregularized systems required a reduction in the integration stepsize to maintain the desired numerical accuracy; the regularized systems do not. During this same period, the regularized variables did not undergo any stepsize changes, thus indicating that the automatic stepsize scaling feature introduced through regularization maintains the desired accuracy during the close approach when numerical difficulties are usually encountered. Furthermore, throughout the entire integration interval, fewer stepsize changes were required for the regularized variables.

An alternative approach to regularization is suggested by the lack of encounters at the lower boundaries for the regularized variables. Since only the upper boundary is encountered, a value of $n < \frac{3}{2}$ (in the transformation $d\tau = r^{-n}dt$) could be selected. This would keep the stepsize from increasing so rapidly with increasing values of the radius and thus would eliminate the decrease in stepsize resulting from an encounter with the upper boundary. Such a value of n would not eliminate the mathematical singularities; however, in most normal cases, the singularities are never encountered anyway. An interesting possibility for numerical integration stepsize control is presented by this concept.

The information presented thus far has been associated with the characteristics of the last trajectory generated by an iteration process, that is, the converged trajectory. It is of interest to know how the four different cases studied are affected by making certain errors in the initial assumptions for boundary conditions (the Lagrange multipliers and terminal time). Information of the number of iterations required and the computer time expended in converging from certain specified initial error percentages in the Lagrange multipliers is presented in Table 3 for the Earth-escape spiral. For economy, all multipliers were considered to be in error by the same percentage for each case studied. The polar coordinates are less sensitive to errors in the initial Lagrange multipliers than are the rectangular coordinates. The regularized variables are less sensitive to erroneous initial conditions than are the unregularized variables.

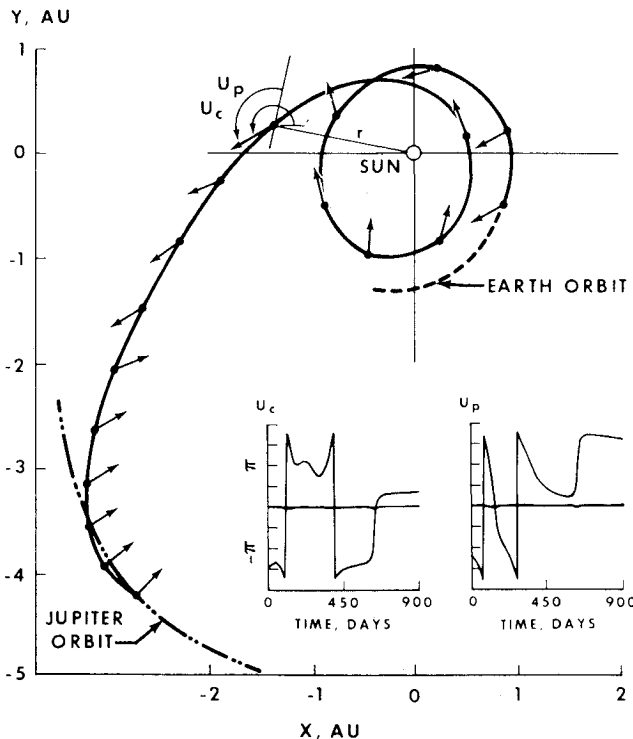


Fig. 4 Optimal Earth-Jupiter trajectory for the launch date of December 1, 1983.

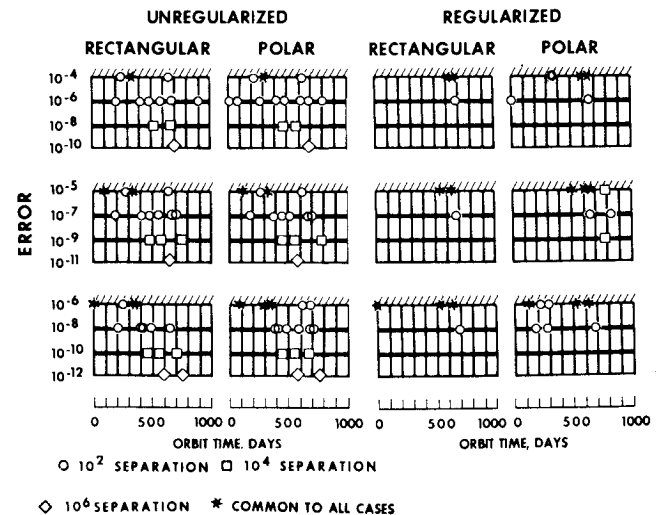


Fig. 5 Integration error-boundary encounters for various error-bound separations for the optimal low-thrust Earth-Jupiter transfer.

Table 2 Earth-Jupiter transfer

	Maximum allowable error (absolute)	Unregularized		Regularized	
		Rectangular	Polar	Rectangular	Polar
Σ sec	10^{-4}	61.7	56.6	51.8	52.1
	10^{-5}	103.6	96.4	54.2	62.5
	10^{-6}	159.7	144.3	106.1	95.6
	10^{-7}	251.2	217.2	206.6	150.2
	10^{-8}	410.9	369.6	219.7	210.8
t_m , msec		0.064	0.062	0.072	0.069
n	10^{-4}	973	908	722	727
	10^{-5}	1615	1530	755	874
	10^{-6}	2512	2282	1474	1341
	10^{-7}	3882	3450	2895	2125
	10^{-8}	6415	6104	3024	3501
m	10^{-4}	3	3	2	2
	10^{-5}	5	5	2	5
	10^{-6}	6	6	3	3
	10^{-7}	5	5	4	4
	10^{-8}	7	7	4	5
$\bar{e}f$	10^{-4}	1.668^{-9}	1.109^{-9}	3.340^{-11}	4.325^{-8}
	10^{-5}	1.768^{-9}	3.386^{-8}	3.439^{-9}	4.994^{-8}
	10^{-6}	2.210^{-11}	3.743^{-9}	2.966^{-11}	8.304^{-10}
	10^{-7}	4.293^{-11}	5.316^{-9}	2.711^{-12}	8.152^{-10}
	10^{-8}	1.454^{-11}	3.589^{-9}	2.192^{-11}	3.725^{-11}

Although the number of iterations required to achieve convergence is essentially the same for all cases, the computer time requirements are smaller for the regularized variables. The reason may be seen from Fig. 6. For initial multiplier errors of 8%, the convergence rate of the regularized variables is greater. The trend presented in Fig. 6 is considered to be representative of all cases given in Table 3. Had Table 3 been expanded to include errors greater than $\pm 20\%$, the computer time savings of the regularized variables would have been more significant. Note that for results presented in Fig. 6 and in Table 3, the value of the terminal time was not changed. Generally, this is not realistic. If the radius vector increases with time and regularized variables are being used, care must be taken in the initial assumption for the terminal time. The sensitivity of the terminal pseudo-time τ to errors in the terminal time t is seen in Fig. 2. One solution involves continuously monitoring the terminal norm and selecting the terminal time which corresponds to the minimum norm for the first assumption.

Although, for some cases, the regularized and unregularized systems may exhibit nearly equal integration times, the integration accuracies may differ. Since a closed-form solution to the problem considered here does not exist, the error generated by the numerical integration process is unknown.

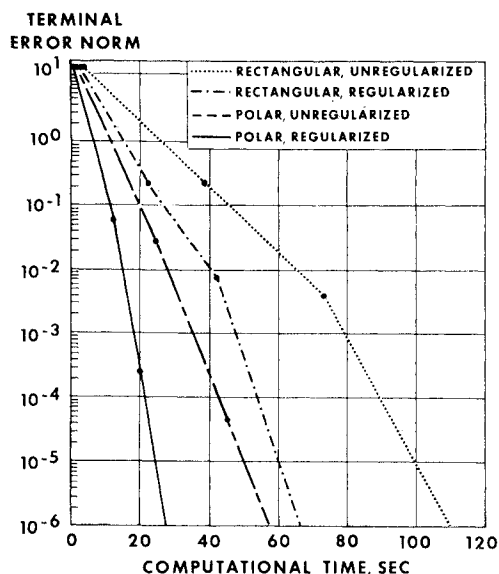


Fig. 6 Terminal error norm compared to computational time for $\delta\lambda_0 = +8\%$ and $dt_f = 0$.

Table 3 Initial error influence on the convergence characteristics of the Earth-escape spiral for unregularized and regularized rectangular and polar coordinates for integration error bounds of 10^{-5} to 10^{-9}

Initial error in λ , %	Unregularized				Regularized			
	Rectangular N^a	Polar t^a	Rectangular N	Polar t	Rectangular N	Polar t	Rectangular N	Polar t
20	6	2.9	5	1.5	6	1.7	5	0.8
16	5	2.3	5	1.5	6	1.7	5	0.8
12	5	2.4	4	1.1	5	1.4	4	0.6
8	5	2.4	4	1.1	5	1.4	4	0.6
4	4	1.8	4	1.1	5	1.4	4	0.6
0	0	0.06	0	0.04	0	0.04	0	0.03
-4	5	2.3	4	1.2	5	1.7	4	0.6
-8	6	2.9	4	1.2	6	1.7	4	0.6
-12	9	4.7	4	1.2	13	4.2	4	0.6
-16	7	3.5	4	1.1	6	1.7	4	0.6
-20	7	3.5	4	1.1	6	1.7	5	0.7

^a N = Iterations required for convergence; t = computation time, min.

However, a constant of motion ($1 + H$) exists, which may be considered in evaluating the accuracy of the numerical integration procedure. This constant of motion, evaluated at the final time, is given by Eq. (5). For the example discussed, $1 + H$ must be zero throughout the trajectory. Thus, the deviation of $1 + H$ from zero is one indication of the error in the numerical integration process. However, satisfaction of $1 + H = 0$ is necessary but is not sufficient to ensure numerical integration accuracy. Since some of the terms in the expression for $1 + H$ contain combinations of the integrated variables, large errors generated in two separate terms could cancel, leaving the impression that high numerical accuracy had been achieved.

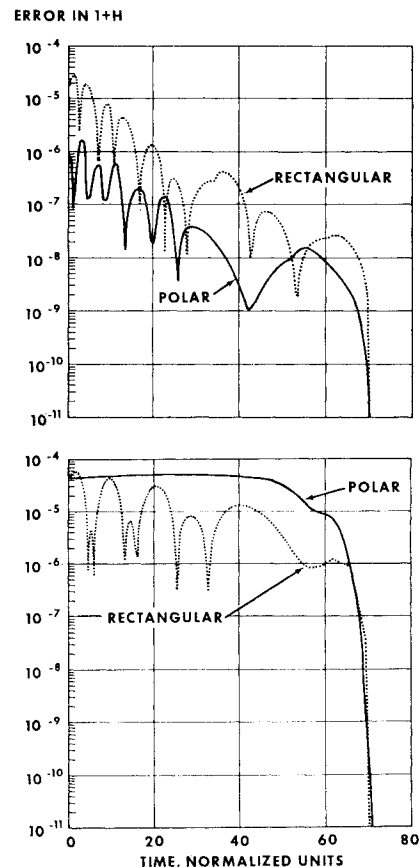


Fig. 7 Error in $1 + H$ for the regularized rectangular and polar coordinates for an error bound of 10^{-5} to 10^{-9} (rectangular coordinates required 497 steps, polar coordinates required 261 steps).

The relative values of $1 + H$ for converged iterations (using the regularized and unregularized systems) may be seen by comparing Figs. 7a and 7b. The error in $1 + H$ is less for the unregularized polar system than for the rectangular system (Fig. 7a), and it is less for the regularized polar system than for the regularized rectangular system (Fig. 7b). However, at the terminal time, the polar coordinate error is less than the rectangular coordinate error. Note also that the error in $1 + H$ for the regularized polar system is relatively constant during most of the integration interval; hence, the automatic stepsize adjustment associated with the regularized variables tends to control the numerical error. For the unregularized variables, the error passes from a relatively large value to a relatively small value during the course of the trajectory (Fig. 7a).

Concluding Remarks

Based on the results obtained in this investigation, the following general conclusions can be drawn. Care in the selection of the coordinate system used to describe an optimal trajectory can lead to increased accuracy and reduced computation time. In addition, for continuously thrusting space vehicles subjected to a gravitational force which undergoes wide variations in the force magnitude, significant reductions in computing time can be achieved by using a regularized form for the equations. In this study, reductions in computing time (by a factor of 3) are obtained in some cases by using regularized variables. In addition, if the Hamiltonian is used as an indication of numerical accuracy, the tradeoff between integration time and integration accuracy is apparent. It is shown that regularization of the variables results in an automatic stepsize change that produces relatively constant numerical error over the trajectory interval. These results indicate the importance of obtaining more

definitive methods for selecting regularizing transformations.

References

- ¹ Tapley, B. D. and Lewallen, J. M., "Comparison of Several Numerical Optimization Methods," *Journal of Optimization Theory and Applications*, Vol. 1, No. 1, July 1967.
- ² Lewallen, J. M., Tapley, B. D., and Williams, S. D., "Iteration Procedures for Indirect Trajectory Optimization Methods," *Journal of Spacecraft and Rockets*, Vol. 5, No. 3, March 1968, pp. 321-377.
- ³ Szebehely, V., Pierce, D. A., and Standis, E. M., Jr., "A Group of Earth-to-Moon Trajectories with Consecutive Collisions," *AIAA Progress in Astronautics and Aeronautics: Celestial Mechanics and Astrodynamics*, Vol. 14, edited by V. G. Szebehely, Academic Press, New York, 1964, pp. 35-52.
- ⁴ Stiefel, E. et al., "Methods of Regularization for Computing Orbits in Celestial Mechanics," CR-769, 1967, Swiss Federal Institute of Technology, NASA.
- ⁵ Tapley, B. D., Szebehely, V., and Lewallen, J. M., "Trajectory Optimization Using Regularized Variables," AIAA Paper 68-099, Jackson, Wyo., 1968.
- ⁶ Schwausch, O. A., "Numerical Error Comparisons for Integration of Near Earth Orbits in Various Coordinate Systems," EMRL 1054, Jan. 1968, The University of Texas, Austin, Texas.
- ⁷ Rainbolt, M. B., "Coordinate System Influence on Numerical Solution of the Trajectory Optimization Problem," Master's thesis, May 1968, Mechanical Engineering Dept., Univ. Houston, Houston, Texas.
- ⁸ McDermott, M. Jr., "Comparison of Coordinate Systems for Numerical Computation of Optimal Trajectories," TR-23, April 1967, Lockheed Electronics Co., Houston, Texas.
- ⁹ Sundman, K. F., "Mémoire sur le Problème des Trois Corps," *Acta Mathematica*, Vol. 36, 1912.
- ¹⁰ Schwausch, O. A., "Subroutine Steper, A Fortran Subroutine for the Numerical Integration of First-Order Ordinary Differential Equations Using Either A Fixed or Variable Integration Step Size," NAS 9-5384, April 1969, Catalog 186, Lockheed Electronics Co., Houston, Texas.